



Science Arts & Métiers (SAM)

is an open access repository that collects the work of Arts et Métiers Institute of Technology researchers and makes it freely available over the web where possible.

This is an author-deposited version published in: <https://sam.ensam.eu>
Handle ID: <http://hdl.handle.net/10985/7382>

To cite this version :

Elena BERGAMINI, Helene PILLET, Jérôme HAUSSELLE, Patricia THOREUX, Sandra GUÉRARD, Valentina CAMOMILLA, Aurelio CAPPOZZO, Wafa SKALLI - Tibio-femoral joint constraints for bone pose estimation during movement using multi-body optimization - Gait and Posture - Vol. 33, p.706–711 - 2011

Any correspondence concerning this service should be sent to the repository

Administrator : scienceouverte@ensam.eu



Tibio-femoral joint constraints for bone pose estimation during movement using multi-body optimization

E. Bergamini^{a,b}, H. Pillet^b, J. Hausselle^b, P. Thoreux^{b,c}, S. Guerard^b, V. Camomilla^{a,*},
A. Cappozzo^a, W. Skalli^b

^a Locomotor Apparatus Bioengineering Laboratory, Department of Human Movement and Sport Sciences, University of Rome "Foro Italico", piazza Lauro De Bosis 15, 00135 Rome, Italy

^b Laboratoire de Biomécanique, Arts et Métiers ParisTech, 151 bd de l'Hôpital, 75013 Paris, France

^c Service de Chirurgie Orthopédique et Traumatologique, Hôpital Avicenne-Université Paris 13, 125 route de Stalingrad, 93009 Bobigny, France

ABSTRACT

When using skin markers and stereophotogrammetry for movement analysis, bone pose estimation may be performed using multi-body optimization with the intent of reducing the effect of soft tissue artefacts. When the joint of interest is the knee, improvement of this approach requires defining subject-specific relevant kinematic constraints. The aim of this work was to provide these constraints in the form of plausible values for the distances between origin and insertion of the main ligaments (ligament lengths), during loaded healthy knee flexion, taking into account the indeterminacies associated with landmark identification during anatomical calibration.

Ligament attachment sites were identified through virtual palpation on digital bone templates. Attachments sites were estimated for six knee specimens by matching the femur and tibia templates to low-dose stereoradiography images. Movement data were obtained using stereophotogrammetry and pin markers. Relevant ligament lengths for the anterior and posterior cruciate, lateral collateral, and deep and superficial bundles of the medial collateral ligaments (ACL, PCL, LCL, MCLdeep, MCLsup) were calculated. The effect of landmark identification variability was evaluated performing a Monte Carlo simulation on the coordinates of the origin-insertion centroids. The ACL and LCL lengths were found to decrease, and the MCLdeep length to increase significantly during flexion, while variations in PCL and MCLsup length was concealed by the experimental indeterminacy.

An analytical model is given that provides subject-specific plausible ligament length variations as functions of the knee flexion angle and that can be incorporated in a multi-body optimization procedure.

Keywords:

Knee ligament length
Joint constraints
Soft tissue artefact
Global optimization
Biomechanics

1. Introduction

Human movement analysis is largely based on the use of skin markers and stereophotogrammetry. Since markers are not rigidly associated with the underlying bone, bone pose reconstruction is affected by a soft tissue artefact. The magnitude of this artefact and its disruptive consequences on the accuracy of the mechanical analysis of a motor act are well described in the literature [1].

In order to compensate for soft tissue artefacts, several techniques have been proposed. All of them exploit redundancy of measured information and embed a model of the artefact [2–4]. These techniques are either used to optimally estimate the pose of one bony segment at a time (single-body optimization), and deal with all of its six degrees of freedom, or aim at optimally estimating

the location in space of a chain of bones interconnected in joints embedding specified constraints (multi-body optimization – MBO; often referred to as global optimization).

As opposed to the single body optimization, which deals only with the artefact deformation of the cluster of markers, the MBO compensates also for its overall displacement relative to the skeleton. In addition, the MBO may provide more realistic joint kinematics by, for instance, preventing bones from appearing to macroscopically pierce into each other. It should be noted, however, that more realistic does not necessarily mean more accurate and that, when using the MBO, the joint degrees of freedom not embedded in the model are sacrificed.

Thus, MBO should not be expected to improve the estimate of joint kinematics [5], but to provide an optimal reconstruction of the instantaneous location in space of the entire chain of bones being analyzed. Therefore, a more accurate kinetic analysis is made possible and the reconstruction of the movement of the soft tissues relative to the underlying bone may be attempted. The latter movement may be fed into a biodynamic model of the human

* Corresponding author. Tel.: +39 06 36733522; fax: +39 06 36733517.
E-mail addresses: valentina.camomilla@uniroma4.it, vcamomilla@tiscali.it (V. Camomilla).

body, the kinetic analysis of which would incorporate the relevant inertial effects that are known to significantly affect the forces involved in motor acts characterized by high accelerations [6]. These considerations justify investing resources aimed at improving the MBO approach.

MBO has been performed mainly using joint constraints which prevent translation, such as spherical, revolute or universal couplings [7,8]. The knee has also been modelled using a parallel mechanism incorporating articular surfaces, as sphere-on-plane contacts, and isometric pseudo-ligamentous structures, and allowing for both translations and rotations [9].

To further improve the quality of these models, it is desirable to develop a subject-specific kinematic model of the human knee which incorporates more realistic non-rigid constraints, based on plausible ranges of the distances between the origin and insertion landmarks (for simplicity, hereinafter referred to as ligament lengths) of the four major ligaments: anterior and posterior cruciate, and lateral and medial collateral ligaments (ACL, PCL, LCL, MCL). It should be noted that the range of such plausible values, in order to be incorporated in the above-mentioned knee model, must account for the indeterminacies associated with the estimation of the subject-specific digital models of the bones involved and of the ligament origin and insertion location (anatomical calibration).

Several authors have focused on ligament kinematic behaviour with the aim to support ligament injury treatment: ACL and PCL elongation was investigated *ex vivo* [10,11] and *in vivo* [12–14]. Fewer studies have dealt with the MCL and LCL [15]. However, most of these studies provide ligament lengths only for a few knee flexion angles and do not display a general consensus about the amount and direction of ligament length variation during flexion. In addition, the errors associated with origin and insertion landmark identification have not been accounted for. Thus, no general boundary conditions, as required in constraint-based knee modelling, can be derived for the ligament lengths during continuous flexion-extension.

The purpose of this study was to determine the above-mentioned plausible values for the ligament lengths during loaded continuous healthy knee flexion. To this aim, *ex vivo* tibio-femoral joints were used to avoid soft tissue artefacts. Three-dimensional digital models of tibias and femura were reconstructed and

ligament attachment areas identified on them together with the associated intra- and inter-operator indeterminacies. The bone models were made to move *in silico* using experimental data obtained on the joint specimens. Ligament lengths were thereafter estimated as a function of the joint flexion angle and submitted to statistical analysis in order to provide a knee joint model that could be embedded in the MBO procedure.

2. Materials and methods

Six knee specimens, consisting of femur, patella, fibula and tibia and intact joint passive structures were harvested from subjects aged 75–96 years old and fresh frozen. They exhibited no advanced osteoarthritis or ligament laxity and presented no recurvatum.

The knee specimens were set in motion using a device described in Azmy et al. [16]. The femur was fixed to the experimental jig and the tibia caused to move by a servo-actuator that applied a force to the quadriceps tendon simulating a contraction of this muscle group. A flexion resistive moment was applied to the knee through two cables fixed to the distal end of the tibia and passing through two pulleys coaxial with the centre of the femoral head and located laterally and medially to it. The force transmitted by these cables to the tibia was equal to 30 N and maintained bone coaptation without damaging the articular structure.

Clusters made of three retro-reflective markers, with a minimal separation of 50 mm, were secured to the femur and to the tibia, each using two pins (Fig. 1a). The marker-cluster 3D positions and orientations were reconstructed during movement using a stereophotogrammetric system (Polaris, Northern Digital Inc., Canada) at a rate of 60 samples per second.

3D digital template models of femur and tibia were obtained from CT-scan images. The perimeters of the origin and insertion areas of the ACL, PCL, LCL, as well as of the deep and superficial bundles of the MCL (MCLdeep, MCLsup), were identified and traced on the bone templates using the mouse pointer (virtual palpation). This procedure was performed seven times by one operator and once by three different operators for a total of ten virtual palpations. The professionals involved were orthopaedic surgeons and underwent a specific and meticulous training.

Two orthogonal digital radiographs of each knee specimen were simultaneously obtained using a low dosage X-ray system (EOS[®],

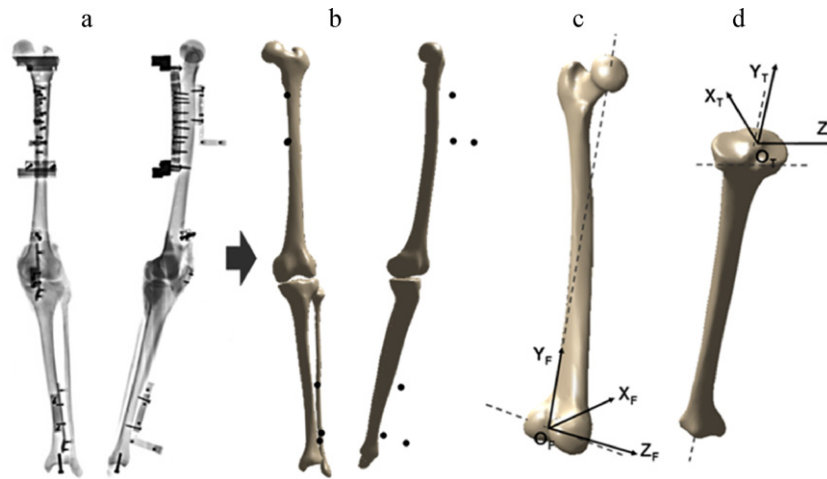


Fig. 1. (a) 2D images acquired with the stereoradiographic system. (b) Reconstruction of the femur and tibia 3D digital models together with the photogrammetric markers. (c) Femur system of reference [18]: O_F (origin): mid point of the segment joining the centres of the two condylar spheres, obtained by least squares approximation of the posterior portion of the medial and lateral epicondyles; Y_F : axis going from O_F to the centre of the femoral head; Z_F : projection onto the plane orthogonal to Y_F of the segment joining the centres of the two condylar spheres (dashed line); X_F : cross product between Y_F and Z_F . (d) Tibia system of reference [18]: O_T (origin): centroid of the tibial plateaux; Y_T : axis going from the centroid of the tibial pilon surface to the intersection between the principal inertial axis of the tibial diaphysis (dashed line) and the tibial plateaux surface; Z_T : projection onto the plane orthogonal to Y_T of the segment joining the most posterior points of the tibial plateaux (dashed line); X_T : cross product between Y_T and Z_T .

EOS-imaging, France) (Fig. 1a). The 3D bone-models were obtained through a reconstruction algorithm based on three steps: (1) identification and labelling of anatomical landmarks on the radiographic images in order to set a parametric simplified subject-specific model; (2) pre-morphing of the bone template to get an initial estimate of the bone; (3) iterative deformation of the latter estimate, based on parametric models and statistical inferences, until the best estimate of the subject-specific bone-model, carrying marks indicating the selected ligament attachment areas, was obtained (Fig. 1b) [17]. The root mean square discrepancy between a digital model of a femur or tibia, as obtained using this procedure, and the relevant CT-scan model, was assessed in a previous study and found to be, on average, less than 1 mm [17]. Each subject-specific bone-model was reconstructed twice by three operators.

Each specimen was subjected to six flexion-extension cycles during which marker trajectories were recorded.

Femur and tibia anatomical frames (Fig. 1c and d) were defined as suggested in Schlatterer et al. [18].

Using the marker coordinates in the EOS[®] frame, the subject-specific bone-models and the relevant anatomical axes were registered with respect to the movement data given in the stereophotogrammetric (global) frame. The knee joint kinematics was then estimated using the Cardan convention and the sequence Z_T, X_T, Y_T .

For each of the six specimens, each knee-model reconstruction, each flexion-extension cycle, and each virtual palpation, the centroids of the attachment areas of each ligament were determined. The mean values and standard deviations (SDs) of these centroid coordinates, as represented in the global frame, were calculated. Virtual palpation did not display any significant difference between inter and intra-operator variability.

The ligament lengths between the mean origin and insertion centroids, obtained averaging the ten virtual palpations, were then computed during the knee movement (d_c) (Fig. 2).

A similarity analysis of d_c vs. flexion angle curves, as obtained from the six flexion-extension cycles, was performed ($r = 0.98 \pm 0.01$; RMSE = 0.15 ± 0.01 mm). Results showed that no significant hysteresis occurred, thus, only mean curves were considered for further analysis.

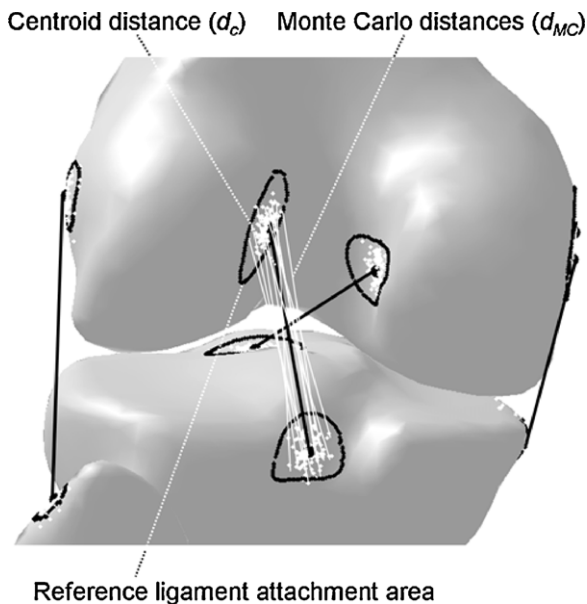


Fig. 2. Digital model of a randomly chosen knee specimen: the ligament attachment areas and the tibio-femoral distances between the centroids (d_c) (black lines) as well as between selected Monte Carlo pairs (d_{MC}) (white lines) are depicted.

At this point, for each knee, the data set was made of six curves, one for each knee-model reconstruction.

In order to assess the impact of the indeterminacy associated with the bone-model reconstruction procedure on the estimation of ligament length, a parametric statistical analysis was carried out by making reference to the d_c values at full knee extension (d_e). To this purpose the intraclass correlation coefficient (ICC) [19] was calculated and the Bland and Altman plots with correlation analysis of the bias between each couple of operators inspected [20].

The propagation to the d_c values of the errors associated with the variability of the virtual palpation was assessed using a Monte Carlo simulation. Origin and insertion points were randomly generated, using a normally distributed mislocation from the mean centroid. The ligament length between each possible pair of the generated origin and insertion points (100×100 pairs) was computed during knee motion (d_{MC}) (Fig. 2).

For the sake of generalization, ligament length variations (Δd_{MC}) were then calculated relative to d_e and expressed as percentage of the latter value for each sampled knee flexion angle. The mean and standard deviation values of Δd_{MC} were then calculated for each Monte Carlo pair over the six specimens and the six digital model reconstructions. To facilitate embedding this information in the knee kinematic model to be used in the MBO procedure, the mean of the Δd_{MC} curves vs. flexion angle thus obtained, plus and minus one SD, were fitted with a polynomial regression function of the fifth order.

3. Results

Both the intra- and inter-operator variability displayed a SD lower than 2 mm for all ligaments with regard to the ligament origin and insertion coordinates on subject-specific knee models. Thus, this value was conservatively used as the SD of the normal distribution used in the Monte Carlo simulation.

With respect to the effect of the indeterminacies associated with the subject-specific bone-model reconstruction on the estimate of d_e , a high intra-operator (ICC = 0.936; confidence interval (CI) [0.894;0.961]) and inter-operator (ICC = 0.974; CI [0.960;0.983]) repeatability was found. Bland and Altman plots and correlation analysis on the residuals confirmed these results. The mean bias and the bias correlation computed between each pair of operators were low, with both CIs spanning the zero value, thus demonstrating that no systematic differences were present among the operators (bias = 0.11 mm; CI [-0.309;0.530]; corr = 0.13; CI [-0.116;0.373]). Given the resulting repeatability, multiple reconstructions from different operators were considered as repeated measures. The variability of d_e over the six observations and averaged over the six knees was measured by a SD equal to 2.3 mm for ACL, 1.9 mm for PCL, 2.4 mm for MCLdeep, 2.1 mm for MCLsup, and 1.7 mm for LCL.

In Fig. 3, the distance d_c is represented against the knee flexion angle with reference to a randomly chosen knee. The ACL, LCL, and MCLdeep displayed consistent trends in all knees, while the PCL and the MCLsup did not. In Fig. 3, the selected knee internal-external rotation and the ab-adduction angles are also depicted vs. the flexion angle. The other knees displayed virtually identical curves.

The mean and SD curves of Δd_{MC} are shown in Fig. 4 for each ligament. The coefficients of the regression functions used to fit the displayed curves are reported in Table 1. The mean of the residual error norm between the fitting function and the original curve was lower than $0.7 \pm 0.4\%$.

4. Discussion

To appropriately define knee joint constraints related to ligament geometry, the subject-specific plausible values of the

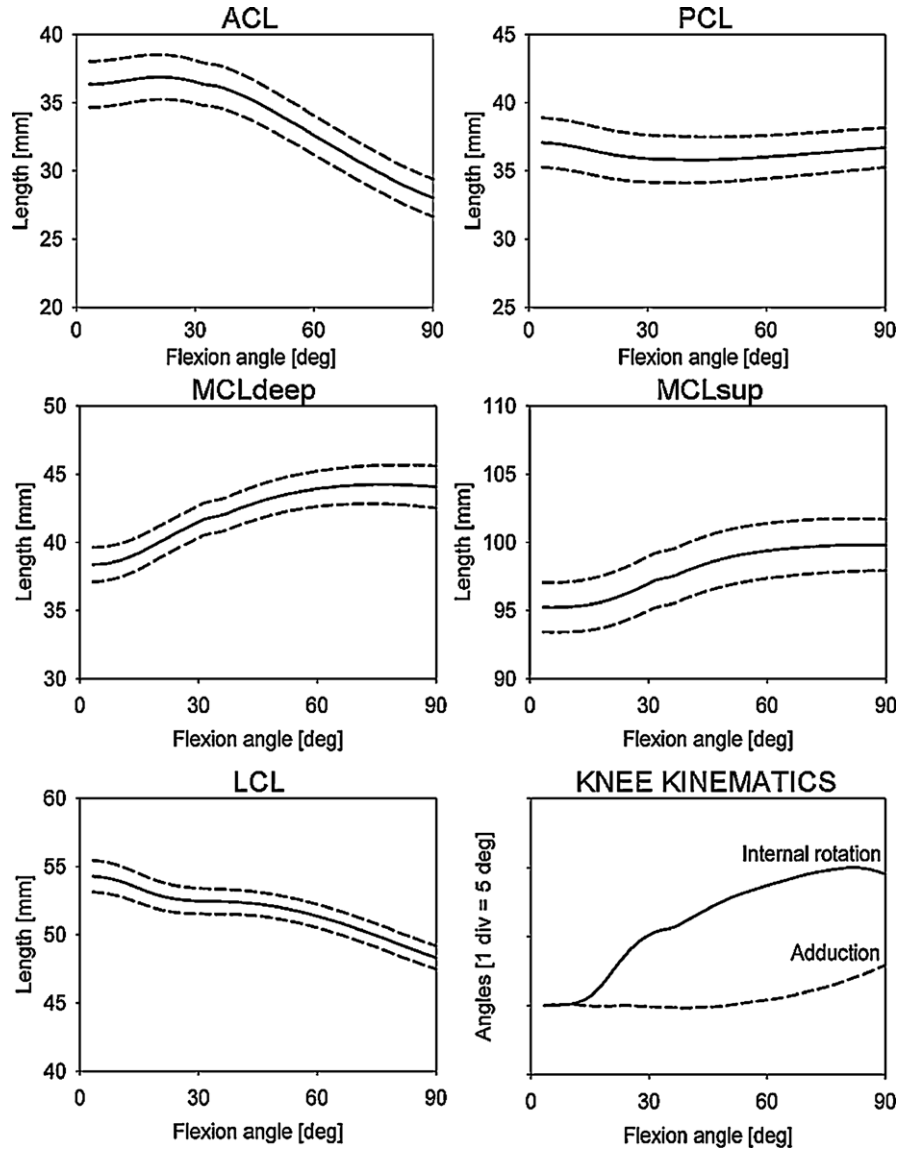


Fig. 3. For one randomly selected knee specimen, the ligament lengths are depicted as a function of the knee flexion angle: mean of three operators times two reconstructions \pm 1SD. The kinematics of the same knee is also shown in the bottom right panel.

lengths of the four major ligaments were assessed during loaded knee flexion, while considering the indeterminacies associated with the estimation of both the subject-specific bone-models and ligament attachment locations.

The ACL and LCL were found to shorten during knee flexion reaching, on average, 22% and 11% of their length at full extension, respectively. This is in agreement with works reporting *in vivo* behaviour of the ACL [12–14,21], *ex vivo* behaviour of the LCL [22] and with a simulation study involving both ligaments [23].

PCL length increased or decreased depending on the selected origin and insertion location. This dependency has been already evidenced *ex vivo* [11,24] and by using a simulation approach [23]. Conversely, *in vivo* studies showed an elongation of the PCL central bundle [25], as well as of the antero-medial and postero-lateral bundles [14]. Since the patterns of ligament length variation depend on the kinematics of the joint [23,26], the lack of agreement between *in vivo* and *ex vivo*, as well as simulation results might be attributed to different amounts of tibial internal rotation during knee flexion, which the referenced papers do not report. *In vivo* knee kinematics was acquired during quasi-static weight-bearing flexion (single-legged lunge using the free leg for

stability). Conversely, during *ex vivo* studies, loaded knee flexion was obtained by applying a force on the fixed femur (to the quadriceps tendon or to the patella, when the patellar ligament was intact) and leaving the tibia free to rotate, or similarly, fixing the tibia and allowing femur rotation.

Results on the deep and superficial bundles of the MCL must be interpreted in the light of the following considerations. First, typical of the MCL is the critical identification of its tibial origin, due to the lack of clear-cut bony prominences [27]. Second, most of the previous studies describe the length of the ligament by a broken line wrapping around the most prominent edge of the tibial plateau [15]. Conversely, in the present work, consistent with the proposed kinematic knee model, the length was computed as a point-to-point distance. The MCLsup length increased or decreased depending on the selected Monte Carlo pairs. This behaviour matches the results obtained *in vivo* by Van de Velde et al. [15] who showed that, during knee flexion, the central, anterior, and posterior bundles exhibited a nearly constant, increasing and decreasing length, respectively. The average tendency of the MCLdeep length to increase during knee flexion, accompanied by a maximal 10% shortening and 20% lengthening of certain Monte

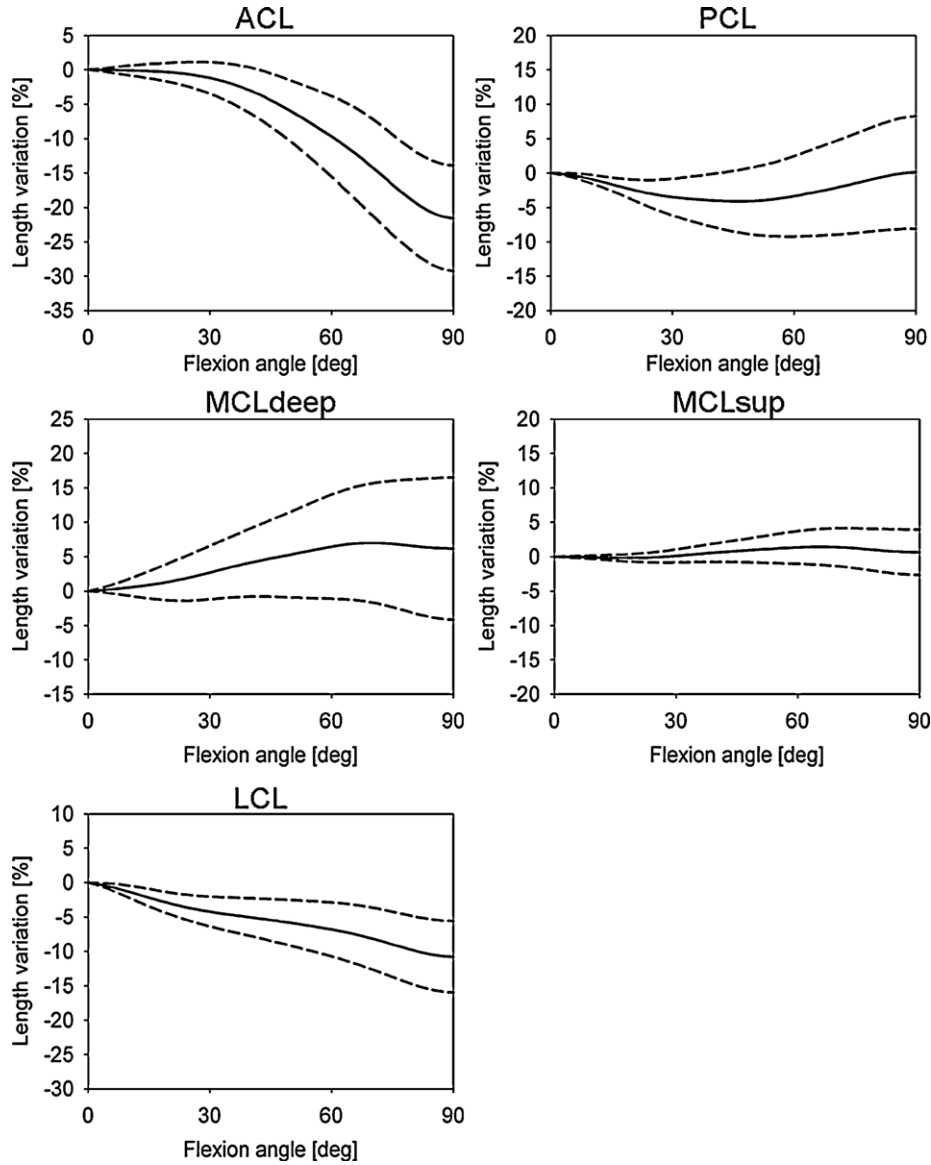


Fig. 4. Distance variation patterns (mean \pm 1SD) vs the knee flexion angle as obtained through the Monte Carlo simulation for each ligament, Δd_{MC} . Each variation is expressed as a percentage of the distance at knee maximal extension, d_e .

Carlo pairs, is in partial agreement with the results reported by Van de Velde et al. [15]. These authors showed that the central bundle does not change significantly its length, while the anterior bundle, on average, has a 10% lengthening and the posterior bundle a 10% shortening.

The expertise and experience of the operators involved in this study is supported by the low intra- and inter-operator variability in the identification of the ligament attachment points, which was less than 2 mm. The Monte Carlo simulation included a wide range of origin-insertion pairs and confirmed the important effects of attachment sites location on ligament length variation. This has been shown previously, however, using fewer origin-insertion points. Feeley et al. [28] considered, for the MCLsup, five points on the femur and four on the tibia, and others [11,29] included less than ten combinations for the ACL and PCL.

Limitations of this study were that the ligaments involved belonged to elderly individuals, with biased mechanical properties, and that an *ex vivo* experimental model was used. It may be assumed however, that *in vivo* joint kinematics of healthy subjects,

under whatever external loading, is not different from the kinematics obtained in this study to an extent that would cause a significant change in ligament length behaviour. In both cases, in fact, stability or coaptation of the joint should be guaranteed, although in a different manner, by a synergic activity of both passive and active intra- and periarticular structures. This hypothesis is supported by recent findings that, during a highly dynamic motion such as the landing phase of a jump, showed that the ACL length decreases during flexion by an amount similar to that obtained in the present study [30].

In conclusion, the results of this study indicate that, in the framework of the MBO approach, a kinematic model of the knee based on joint constraints should consider the length of ACL, LCL and MCLdeep variable as a function of knee flexion. Given the dependence of PCL and MCLsup length variation from the selected attachment sites, these ligaments could be considered isometric. The efficacy of this kinematic model, as opposed to those already implemented, must be evaluated in terms of consequences on the estimate of joint kinetics, particularly when the inertial effects of soft tissue masses are involved.

Table 1

Coefficients of the fifth-order polynomial regression function used to fit the mean and SD distance curves obtained from the Monte Carlo pairs (see Fig. 4): d (dependent variable): percentage ligament length variation [%]; β (independent variable): knee flexion angle [deg].

		a_0	a_1	a_2	a_3	a_4	a_5
ACL	Mean	-4.3	-7.4	-3.9	-0.1	0.5	0.1
	+1SD	-0.4	-4.1	-3.5	-0.6	0.4	0.2
	-1SD	-8.2	-10.7	-4.3	0.4	0.7	0.1
PCL	Mean	-4.1	0.1	2.4	0.0	-0.3	0.0
	+1SD	0.2	2.9	2.1	0.0	-0.2	-0.1
	-1SD	-8.5	-2.7	2.7	-0.1	-0.4	0.1
MCLdeep	Mean	4.8	3.6	-0.8	-0.9	0.1	0.1
	+1SD	10.4	6.8	-0.7	-0.9	-0.1	0.1
	-1SD	-0.9	0.4	-0.9	-1.0	0.2	0.1
MCLsup	Mean	0.8	1.3	-0.3	-0.7	0.0	0.1
	+1SD	2.4	2.6	-0.2	-0.9	0.0	0.1
	-1SD	-0.8	0.0	-0.4	-0.5	0.1	0.1
LCL	Mean	-5.4	-1.9	-0.2	-1.2	0.1	0.2
	+1SD	-2.4	-0.4	-0.1	-1.1	0.0	0.2
	-1SD	-8.5	-3.4	-0.3	-1.2	0.2	0.3

In order to improve the fitting model accuracy and to reduce the influence of random errors on the regression coefficients, the independent variable β was standardized by computing its z-score, using its mean (μ) and the corresponding standard deviation (σ): $z = \frac{(\beta - \mu)}{\sigma}$ where $\mu = 45$ deg. and $\sigma = 26$ deg. The following regression equation was then used $d = a_0 + a_1z + a_2z^2 + a_3z^3 + a_4z^4 + a_5z^5$.

Acknowledgements

The financial support of the Università Italo-Francese (Call Vinci) and of the Department of Human Movement and Sport Sciences of the University of Rome “Foro Italico” is gratefully acknowledged. The authors wish to acknowledge Dr. Sophie Lacoste for her technical support and John McCamley for his contribution to the refinement of the manuscript.

Conflict of interest: The authors do not have any financial or personal relationships with other people or organizations that could inappropriately influence the manuscript.

References

- [1] Peters A, Galna B, Sangeux M, Morris M, Baker R. Quantification of soft tissue artifact in lower limb human motion analysis: a systematic review. *Gait Posture* 2010;31:1–8.
- [2] Soderkvist I, Wedin PA. Determining the movements of the skeleton using well-configured markers. *J Biomech* 1993;26(12):1473–7.
- [3] Chèze L, Fregly BJ, Dimnet J. A solidification procedure to facilitate kinematic analyses based on video system data. *J Biomech* 1995;28(7):879–84.
- [4] Alexander EJ, Andriacchi TP. Correcting for deformation in skin-based marker systems. *J Biomech* 2001;34(3):355–61.
- [5] Andersen MS, Benoit DL, Damsgaard M, Ramsey DK, Rasmussen J. Do kinematic models reduce the effects of soft tissue artefacts in skin marker-based motion analysis? An *in vivo* study of knee kinematics. *J Biomech* 2010;43(2):268–73.
- [6] de Leva P, Cappozzo A. Estimating forces in sport biomechanics. In: Rainoldi A, Minetto MA, Merletti R, editors. *Biomedical engineering in exercise and sports*. Turin (IT): Edizioni Minerva Medica; 2006. p. 71–88.
- [7] Lu TW, O'Connor JJ. Bone position estimation from skin marker co-ordinates using global optimization with joint constraints. *J Biomech* 1999;32:129–34.
- [8] Andersen MS, Damsgaard M, Rasmussen J. Kinematic analysis of over-determinate biomechanical systems. *Comp Meth Biomech Biomed Eng* 2009;12(4):371–84.
- [9] Duprey S, Cheze L, Dumas R. Influence of joint constraints on lower limb kinematics estimation from skin markers using global optimization. *J Biomech* 2010;43(14):2858–62.
- [10] Hollis JM, Takai S, Adams DJ, Horibe S, Woo SLY. The effects of knee motion and external loading on the length of anterior cruciate ligament (ACL): a kinematic study. *J Biomech Eng* 1991;113:208–14.
- [11] Grood ES, Hefzy MS, Lindenfield TN. Factors affecting the region of most isometric femoral attachments: part I: the posterior cruciate ligament. *Am J Sports Med* 1989;17(2):197–207.
- [12] Yoo YS, Jeong WS, Shetty NS, Ingham SJM, Smolinski P, Fu F. Changes in ACL length at different knee flexion angles: an *in vivo* biomechanical study. *Knee Surg Sport Tr A* 2010;18(3):292–7.
- [13] Hosseini A, Gill TJ, Li G. *In vivo* anterior cruciate ligament elongation in response to axial tibial loads. *J Orthop Sci* 2009;14(3):298–306.
- [14] Li G, DeFrate LE, Sun H, Gill TJ. *In vivo* elongation of the anterior cruciate ligament and posterior cruciate ligament during knee flexion. *Am J Sports Med* 2004;32(6):1415–20.
- [15] Van de Velde SK, DeFrate LE, Gill TJ, Moses JM, Papannagari R, Li G. The effect of anterior cruciate ligament deficiency on the *in vivo* elongation of the medial and lateral collateral ligaments. *Am J Sports Med* 2007;35(2):294–300.
- [16] Azmy C, Guérard S, Bonnet X, Gabrielli F, Skalli W. EOS[®] orthopaedic imaging system to study patellofemoral kinematics: assessment of uncertainty. *Orthop Traum Surg Res* 2010;96(1):28–36.
- [17] Chaibi Y, Cressonb T, Aubert B, Hausselle J, Neyret P, Hauger O, de Guise JA, Skalli W. Fast 3D reconstruction of the lower limb using a parametric model and statistical inferences and clinical measurements calculation from biplanar X-rays. *Comp Meth Biomech Biomed Eng*; 2010;[doi:10.1080/10255842.2010.540758](https://doi.org/10.1080/10255842.2010.540758).
- [18] Schlatterer B, Suedhoff I, Bonnet X, Catonne Y, Maestro M, Skalli W. Skeletal landmarks for TKR implantations: evaluation of their accuracy using EOS imaging acquisition system. *Orthop Traum Surg Res* 2009;95(1):2–11.
- [19] McGraw KO, Wong SP. Forming inferences about some intraclass correlation coefficients. *Psychol Meth* 1996;1(1):30–46.
- [20] Bland JM, Altman DJ. Statistical methods for assessing agreement between two methods of clinical measurement. *Lancet* 1986;1(8476):307–10.
- [21] Beynon BD, Uh BS, Johnson RJ, Fleming BC, Renström PA, Nichols CE. The elongation behavior of the anterior cruciate ligament graft *in vivo*—a long-term follow-up study. *Am J Sports Med* 2001;29(2):161–6.
- [22] Harfe DT, Chuinard CR, Espinoza LM, Thomas KA, Solomonow M. Elongation patterns of the collateral ligaments of the human knee. *Cl Biomech* 1998;13(3):163–75.
- [23] Amiri S, Cooke D, Kim IY, Wyssset U. Mechanics of the passive knee joint. Part 2: interaction between the ligaments and the articular surfaces in guiding the joint motion. *Proc Inst Mech Eng H* 2007;221(8):821–32.
- [24] Ahmad CS, Cohen ZA, Levine WN. Codominance of the individual posterior cruciate ligament bundles: an analysis of bundle lengths and orientation. *Am J Sports Med* 2003;31:221–5.
- [25] DeFrate LE, Gill TJ, Li G. *In vivo* function of the posterior cruciate ligament during weightbearing knee flexion. *Am J Sports Med* 2004;32(8):1923–8.
- [26] Woo SLY, Debski RE, Withrow JD, Jansushak MA. Biomechanics of knee ligaments. *Am J Sports Med* 1999;27(4):533–43.
- [27] Liu F, Yue B, Gadikota HR, Kozanek M, Liu W, Gill TJ, Rubash EA, Li G. Morphology of the medial collateral ligament of the knee. *J Orthop Sur Res* 2010;5(1):69–77.
- [28] Feeley BT, Muller MS, Allen AA, Granchi CC, Pearle AD. Isometry of medial collateral ligament reconstruction. *Knee Surg Sport Tr A* 2009;17(9):1078–82.
- [29] Schutzer SF, Christe S, Jacob RP. Further observations on the isometricity of the anterior cruciate ligament: an anatomical study using a 6-mm diameter replacement. *Clin Orthop Relat Res* 1989;242:247–55.
- [30] Taylor KA, Terry ME, Utturkar GM, Spritzer CE, Queen RM, Irribarra LA, Garrett WA, DeFrate LE. Measurement of *in vivo* anterior cruciate ligament strain during dynamic jump landing. *J Biomech* 2011;44:365–71.